

This item was submitted to [Loughborough's Research Repository](#) by the author.
Items in Figshare are protected by copyright, with all rights reserved, unless otherwise indicated.

Textile-based sensors for electrical current measurement in three-phase cables

PLEASE CITE THE PUBLISHED VERSION

<https://doi.org/10.1049/stg2.12047>

PUBLISHER

John Wiley & Sons Ltd on behalf of The Institution of Engineering and Technology

VERSION

VoR (Version of Record)

PUBLISHER STATEMENT

This is an Open Access Article. It is published by Wiley under the Creative Commons Attribution 4.0 Unported Licence (CC BY). Full details of this licence are available at: <http://creativecommons.org/licenses/by/4.0/>

LICENCE


CC BY 4.0

REPOSITORY RECORD

Strickland, Dani, Tincuta Heinzl, Bee King, Mina Abedi-Varnosfaderani, A Zeidler, and Rob Seager. 2021. "Textile-based Sensors for Electrical Current Measurement in Three-phase Cables". Loughborough University. <https://hdl.handle.net/2134/15336405.v1>.

ORIGINAL RESEARCH PAPER

Textile-based sensors for electrical current measurement in three-phase cables

Dani Strickland¹ | Tincuta Heinzl¹ | Bee King¹ | Mina Abedi Varnosfaderani¹  | Alana Zeidler² | Rob Seager¹

¹Wolfson School, Loughborough University, Loughborough, UK

²School of Mechanical Engineering, Leeds University, Leeds, UK

Correspondence

Mina Abedi Varnosfaderani, Wolfson School, Loughborough University, Epinal Way, Loughborough, LE11 3TU, UK.
Email: Abedi-Varnosfaderani@lboro.ac.uk

Funding information

Loughborough University, Grant/Award Number: EPSRC EP/N032888/1

Abstract

There is much discussion about the implementation and benefits of smart electricity networks. However, the reality is that the instrumentation needed at low voltage is too expensive for large-scale deployment. The most highly used monitoring systems in use today are based on Rogowski coil technology, which can only be used on single-phase cables and terminations at £1k–£2k per substation. This study presents the results of novel research into modelling and analysis of a low-cost sensor which can measure load on a 3 core cable at <£150 per substation. This study uses a new textile-based sensor that can be produced by low-cost, high-volume manufacturing techniques. The study describes the modelling that is required in conjunction with the sensor geometry to be able to calculate the load current. Three textile-based sensors of different dimensions were produced and tested and the results were compared with the current probe readings. The study shows that the textile sensors have an offset error of 14% but good linearity of 0.998, for around 10% of the cost of Rogowski coil technology.

1 | INTRODUCTION

The UK government needs to reduce CO₂ emissions by increasing the use of electric vehicles, heat pump usage and distributed renewable generation. Currently, there is very little monitoring below 11 kV in the UK, so it will be difficult to understand the impact of these future changes on the low-voltage network. For many sites, 132 kV/11 kV substation monitoring is commercially available. However, the range of real time systems currently on the market for 11 kV/400 V substations, eMS [1], GridKey [2], Nortech [3], Siemens, Sentient Energy, Ash Wireless and EA Technology, typically cost £1000–£2000 per substation. This is too expensive for large-scale roll out. Western Power Distribution have estimated that for wide-scale deployment, monitoring needs to have a price point of around £150 per substation including installation.

Low-cost substation monitoring has the potential to deliver many benefits, including the following:

- release of thermal capacity of the existing assets on the network
- identifying overloading and other faults before failure

- improved response to outages
- avoiding network reinforcements, saving cost, time and environmental impact
- gaining access to the loading profiles on the network for better and faster turnaround on connection applications
- automatic load and loss minimisation reconfiguration
- input for sparse state estimation for otherwise unmonitored assets

Many distribution substations are more than 40 years old, so any device must be small and capable of non-invasive installation for retrofitting on a wide range of substation and cable types. Current technology is based on the use of a Rogowski coil, which can only be used on single-phase cables. Therefore, to fully understand the load on a substation transformer requires that all of the phases of all of the low-voltage circuits (maybe as many as 15–18) need to be monitored, hence the high cost of current systems. Monitoring a single three-phase cable to the transformer instead of each single-phase wire coming from the transformer would be one way of reducing costs. The aim of this study is to present a method that can be used to measure the load on a 11 kV/400 V

This is an open access article under the terms of the Creative Commons Attribution License, which permits use, distribution and reproduction in any medium, provided the original work is properly cited.

© 2021 The Authors. *IET Smart Grid* published by John Wiley & Sons Ltd on behalf of The Institution of Engineering and Technology.

substation within the £150 per substation price point. The method is designed to produce average loading at a substation between 10-s and 15-min intervals to minimise communication data costs.

There have been several recent developments regarding the methods of measuring load current in three-phase systems. This has included the measurement of loading on both dc [4] and ac [5–9] overhead lines (OHL) using arrays of sensors. In dc systems, it is not possible to use coils of wire to detect the dc field, so an array of tunnelling magnetoresistance (TMR) sensors was used to sense the magnetic field and back calculate the current [4]. References [5–7] also used TMR sensors but to estimate ac loading and the sag on three-phase OHL. TMR sensors were used on three-phase conductors in a planar position as opposed to using as an array distant from the OHL [8]. Alternatives to TMR include air-cored coils [9]. In this work, four coils were used to measure the loading on a horizontal OHL. Three of the coils are placed parallel and one perpendicular to the cross arm. An expression for the induced voltages in the coils due to the currents in the conductor are derived from the geometry and the currents are then back calculated by substitution to obtain complex expressions for the load currents in relation to the measured voltages and geometry. Four coils are used to account for the requirement that the distance between the coil and the conductor is unknown.

An alternative to an air coil has been trialled using a coil with a ferrite centre [10]. Non-linear curve fitting is used to determine the short circuit current of the coil near a conductor. Two of these coils are then used in differential mode to reduce errors to far fields. The work presented in References [4–10] is useful for understanding how multi-array solutions of induced emf in coils can be decomposed into the phase current measurement, which is highly relevant to future development of the work presented in this study.

In addition to OHL measurement, magnetic field sensors have also been used on three-phase busbar arrangements. Hall effect sensors [11, 12] and a planar Rogowski coil current transducer, which, instead of forming a closed loop around the busbar, measures the magnetic field at a point near the busbar [13, 14] have also been trialled. These alternative techniques for measuring load at a substation would require intrusive installation, increasing installation cost above the price point.

Load estimation has been undertaken in more recent years on multi-core cables. Examples include the use of arrays of PCB mounted sensors around the core of the cable [15–21], References [14, 16] reverse calculate the current based on a least fit squares method to relate the calculated magnetic field based on a perceived set of load currents to the measured magnetic field produced by the load current to be determined. Reference [17] extended their analysis using a least square inversion method and using Hall effect sensors on printed PCB material at three different radii. References [18–21] used an array of magneto-resistive sensors with known conductor geometry located around the sensor to give an estimate of the magnetic field. These sensor array designs contained between 8 and 24 sensors per system.

An issue with printed PCBs with arrays of sensors is that they tend to be rigid; if they are multi-level, then they could extend significantly beyond the edges of the cable. This makes them unsuitable for a large proportion of substations where space is an issue, but the work on dealing with current arrays and measurement uncertainty is of future value to the sensor described in this study. Some consideration has been given to flexible, and thin materials. Reference [22] used a printed thin film to generate an array of current sensors for use around a single core cable as a direct substitute for a Rogowski coil. Large numbers of sensors are required for measuring a substation loading.

References [23, 24] developed a new form of coil to wrap around a cable to look at induced emf. Printed flexible circuit boards, wound wire and conductive thread on material were used to manufacture the sensors. However, thin printed film would also have worked. This methodology assumed that the coils of wire in the sensor were located at a single point in space. The reality is that the turns of wire will be distributed due to the thickness of the wire, the requirement to include insulation and the constraints of the manufacturing methodology, for example, minimum tolerance distances to avoid short circuiting the conductive thread.

The research presented in this study is novel because it uses a low-cost, flexible textile sensor to estimate load current on a three-phase cable. The sensor is manufactured in a way that is compatible with large-scale manufacturing processes (the use of industrial embroidery machines—in this case a Brother PR1050x 10-needle embroidery machine was used to stitch out). The sensor measurements are used in conjunction with a model-based method to take account of finite distances between sensor turns to make an indirect measurement of load current. Neumann's formula was used within the model because the measurement device cannot be considered to be located at a single location due to embroidery machine tolerances. The work presented in this study uses conductive thread embroidered onto fabric from different templates with different numbers of turns as an example of an extreme case of distributed coil turns. Conductive thread in textiles is not new and has previously been used in robotics [25], the production of antennas [26, 27], sensors [28, 29] and interaction design [30] but not for load measurement. Section 2 of this study looks at the current theory and describes a new methodology using the Neumann method to deal with distributed turns on a coil. Section 3 describes the experimental setup; Section 4 compares the theoretical and experimental results.

2 | THEORY

2.1 | Existing methodology

The coil works on the same principle as an induction motor under the locked rotor condition, but the 'rotor' part is inverted and located outside of the 'stator' part. Figure 1 shows the flux produced by a three-core cable which looks similar to that in a two-pole machine which rotates with time. Placing a coil axially on the cable causes the time-varying normal

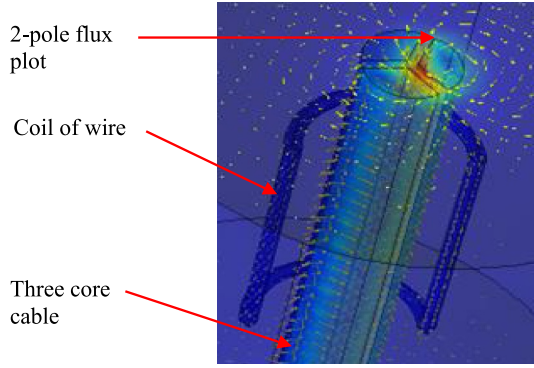


FIGURE 1 The field produced by a three-core cable and a coil of wire to detect the field by induction

component of magnetic field to induce an emf in the coil. This works differently from a Rogowski coil as the normal component of emf is induced in the axial direction of the cable.

In previous work, the coil of wire is assumed to be located axially along the cable at a single position. The induced emf in the coil can be estimated using Faraday's law (1) where e is the induced voltage in the coil of wire (volts), N is the number of turns in the coil and φ is the flux (Wb):

$$e = -N \frac{d\varphi}{dt} \quad (1)$$

If it is assumed that the flux density, B , is changing sinusoidally around the conductor as per (2), then the induced emf in each half of the coil can be calculated from (3) and summed to give a total emf over each co-located turn:

$$B = \hat{B} \sin(\omega t + \theta) \quad (2)$$

where $\omega = 2\pi f$ (rad) and f is the frequency of the supply.

$$e = -N\omega d_2 l \hat{B} \cos(\omega t + \theta) \quad (3)$$

where d_2 [m] is the distance to the coil from the centre of the cable and l is the length of the coil [m].

As this research is in preliminary stages, it is assumed, in this case, that the currents in the cable are balanced. Under this assumption and treating the coil as a point-source sensor, an estimate of current can be made by assuming the current is a point source at the centre of each sector. Figure 2 is used to back calculate the current. In [22, 23], the coil was represented as the single point source aligned with the red phase.

The normal component of flux density at each end of the coil due to the currents in each of the three phases can be derived. This allows the peak emf, \hat{e} , to be estimated leading to an estimate of peak current, \hat{I} , in each phase as shown in (4). Distances d_1 to d_5 (m) are shown in Figure 2:

$$I = \frac{\hat{e}}{3Nf d_2 (d_1 + d_3) l \mu_o \left(\frac{1}{d_4^2} + \frac{1}{d_5^2} \right)} \quad (4)$$

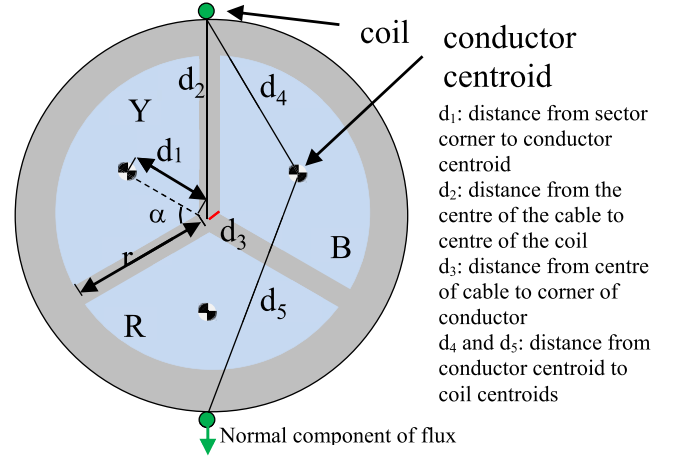


FIGURE 2 A picture of a cross section through a conductor with a coil on the outside with key parameters marked

However, the coil is not a point source and may be distributed over an area. This is particularly true of a coil implemented as a textile where it is necessary to ensure that there is isolation between each line of thread.

In this research study, three coils of different numbers of turns are used to illustrate the methodology. An example coil geometry is shown in Figure 3. Any suitable conductive thread can be used. In this study, Madeira HC40 <300 Ω /m silver-plated polyamide was sewn onto medium-weight calico using a Brother PR1050x 10-needle embroidery machine. Other embroidery substrates could be used, for example, Cordura fabrics, known for its water resistance. Other threads used include Madeira embroidery polyester threads.

The cross sections of the coils as they are located on the cable are shown in Figure 4. These were drawn in Adobe Illustrator and vectorised for use with the embroidery machine software (Wilcom E4). These were stitched out on an embroidery machine; as a result, the distances between the coil turns are slightly different. The as-sewn measurements are used in all the following calculations. It is clear to see that the coils locations are well distributed around the conductor surface compared with the idealistic point source in Figure 2.

The method behind Equation (4) can be adapted such that the calculated magnetic field due to each current on each coil can be calculated based on the geometry. However, this results in a complicated back calculation of current without the advantages of being able to cancel the red phase current.

2.2 | Neumann-based methodology

To overcome the issues with the existing methodology, a method of calculating the mutual inductances between the coil and each of the conductors is undertaken as an alternative.

Neumann-based modelling has been used for complex geometries such as the end-windings of electric machines [31] to more recent applications such as mutual inductance

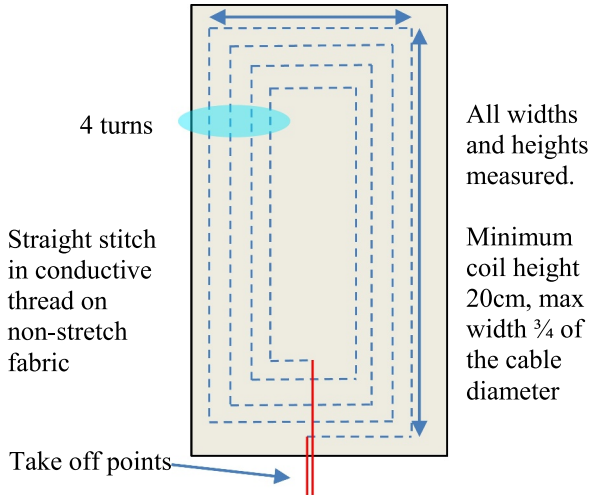


FIGURE 3 A sketch of the coil geometry showing four turns

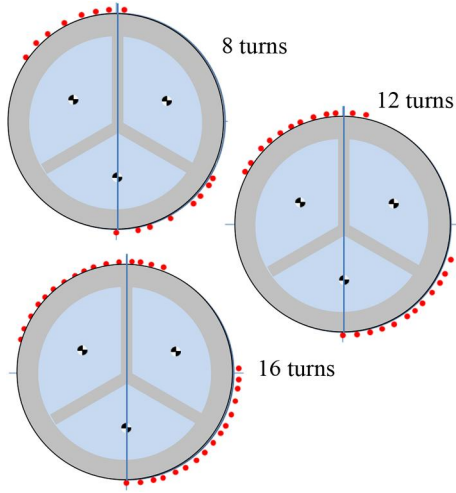


FIGURE 4 A sketch of the three-core sector cable and the radial location of each coil turn on the three samples in relation to the conductor cores

calculation between planar PCBs [32] and copper tracks for contactless energy transfer (CET) [33] and the fundamental equation is shown in (5). Finite element methods can be used but are slow to implement in three dimensions. The coil and the conductor are modelled as filamentary elements in air as shown in Figure 5:

$$M_{cond,coil} = \frac{\mu_0}{4\pi} \oint_{l_{cond}} \oint_{l_{coil}} \frac{dl_{cond} \cdot dl_{coil}}{r} \quad (5)$$

where $M_{cond,coil}$ is the mutual inductance between a conductor and a coil, dl_{cond} is a small element of conductor length, dl_{coil} is a small element of coil length and r is the distance between the two small elements.

The coil and conductor are divided into a large number of filaments and the double integral is replaced by a double summation over each filament.

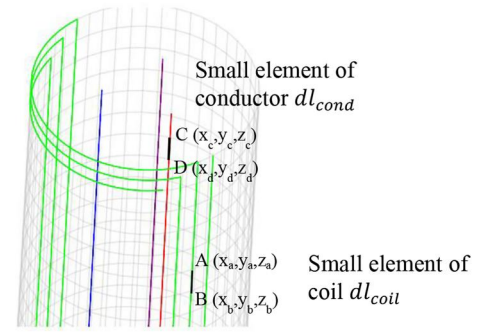


FIGURE 5 A sketch of a coil and conductor filamentary structures showing a filament of current in the conductor and a filament in the coil

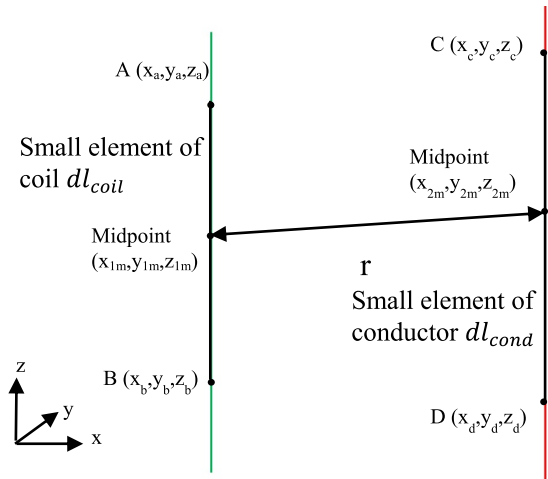


FIGURE 6 A close-up image of the two filaments from the conductor and coil with details of the two vector elements dl_{cond} and dl_{coil}

$$M_{coil,cond} = \frac{\mu_0}{4\pi} \sum_{l_{cond}} \sum_{l_{coil}} \frac{dl_{cond} \cdot dl_{coil}}{r} \quad (6)$$

By looking more closely at the two vector elements dl_{coil} and dl_{cond} as shown in Figure 6, the element length can be found by subtracting the coordinates at the elements end, labelled point A/B and C/D, respectively,

$$dl_{coil} = A - B = [x_a - x_b, y_a - y_b, z_a - z_b] \quad (7)$$

re-labelling the coil lengths in each direction, x_{11}, y_{11}, z_{11}

$$dl_{coil} = [x_{11}, y_{11}, z_{11}] \quad (8)$$

$$dl_{cond} = C - D = [x_c - x_d, y_c - y_d, z_c - z_d] \quad (9)$$

re-labelling the conductor lengths in each direction, x_{12}, y_{12}, z_{12} .

$$dl_{cond} = [x_{12}, y_{12}, z_{12}] \quad (10)$$

The product $dl_{cond} \cdot dl_{coil}$ can therefore be written as follows:

$$dl_{cond}.dl_{coil} = x_{11}x_{12} + y_{11}y_{12} + z_{11}z_{12} \quad (11)$$

r is the distance between element midpoints from Figure 6 giving

$$r = \sqrt{(x_{1m} - x_{2m})^2 + (y_{1m} - y_{2m})^2 + (z_{1m} - z_{2m})^2} \quad (12)$$

$M_{coil,cond}$ can be calculated between the coil and any of the three conductors (M_{RC} , M_{YC} and M_{BC} as the mutual inductance between coil and red, yellow and blue phases, respectively) provided the geometry is known.

Once the mutual inductances are calculated, the induced emf can be obtained from these using (13).

$$e = M_{RC} \frac{dI_R}{dt} + M_{YC} \frac{dI_Y}{dt} + M_{BC} \frac{dI_B}{dt} \quad (13)$$

where I_R , I_Y and I_B are the conductor currents.

Under balanced sinusoidal current conditions, the current peak magnitude, \hat{I} can be estimated as follows:

$$\hat{I} = \frac{\hat{e}}{\omega \sqrt{\left(M_{RC} - \frac{1}{2}M_{YC} - \frac{1}{2}M_{BC}\right)^2 + \left(\frac{\sqrt{3}}{2}M_{YC} - \frac{\sqrt{3}}{2}M_{BC}\right)^2}} \quad (14)$$

For the purposes of the calculation, the conductor length is set to be 2 m long and is split into 200 filaments while each turn in the coil is set to its measured length and is broken up into 90 filaments. The midpoint of the coil occurs at 1 m along the conductor. This number of filaments offers good compromise between accuracy and time. It was determined by increasing the number of filaments until the calculated mutual inductance converged to a fixed value.

3 | EXPERIMENTAL METHOD

To measure the current in a three-phase cable in a substation, it is necessary to have a three-phase supply with the currents present that would typically be seen in a substation. Within the laboratory, it is not possible to have these currents at the voltage levels that would be seen in a substation, thus a laboratory alternative that allows the high currents without the high voltages was used. A three-phase, 45 kVA air-cooled transformer with variable voltage supply was connected to a step down transformer which can supply up to 300 A pk-pk current into a shorted three-phase cable as shown in Figure 7. A three-core 415 V, 95 mm² XLPE cable with outside diameter of 33 mm and grounded sheath was connected and the electromagnetic field measured with the sensors are under test. Experimental hardware is shown in Figure 8 and key data and experimental parameters are in Table 1.

The sensor uses an observable quantity (the measured emf) in conjunction with a mathematical construct (the mutual inductance) to give an indirect measurement of the load current.

Test current generation

A variac is manually adjusted to give a low voltage at the cable terminals which drives a current of between 0A and 106A rms into an electric short circuit.

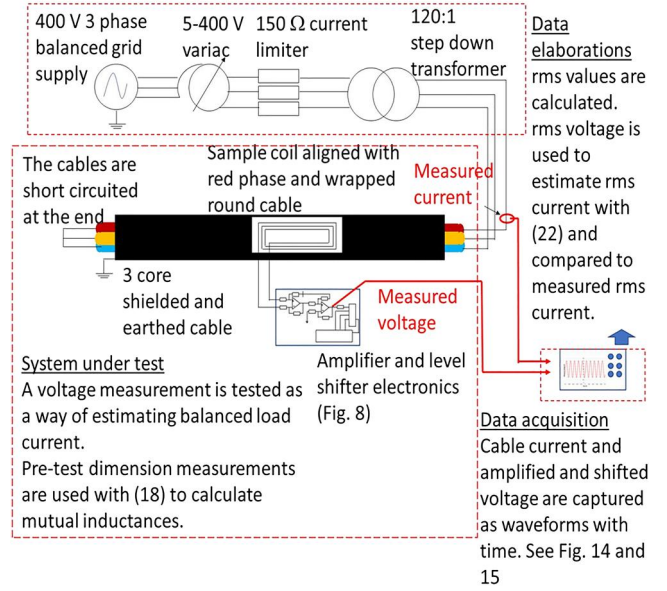


FIGURE 7 A schematic of the test rig

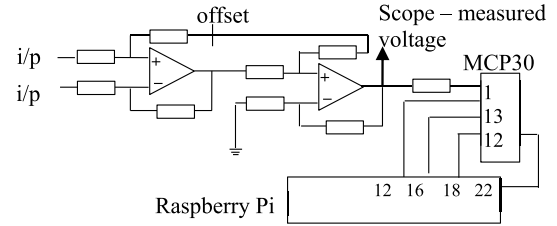


FIGURE 8 A simplified schematic of the electronic signal conditioning circuit

TABLE 1 Key data and experimental parameters

Parameter	Range
Current range	0–150 A rms
Frequency	50 Hz (grid frequency)
Turns in coil samples	8, 12 and 16
Average length and height of 8-turn coil	218 × 50.5 mm
Average length and height of 12-turn coil	213 × 50 mm
Average length and height of 16-turn coil	203 × 47 mm
Voltage amplification	46

This is directly compared with the measured value of load current through a clip on a CP0150 Current Probe. The output of the sensor was connected to a level shifter and an amplifier (x46), so that it can be used in conjunction with a Raspberry Pi.

An op-amp-based circuit in Figure 9 was used to amplify the signal to a more readable value and it is to be level shifted, so that the waveform was >0 V (this is to ensure it works with different processors as some processors only accept 0–5 V inputs). The resultant waveform can be sent to an analogue

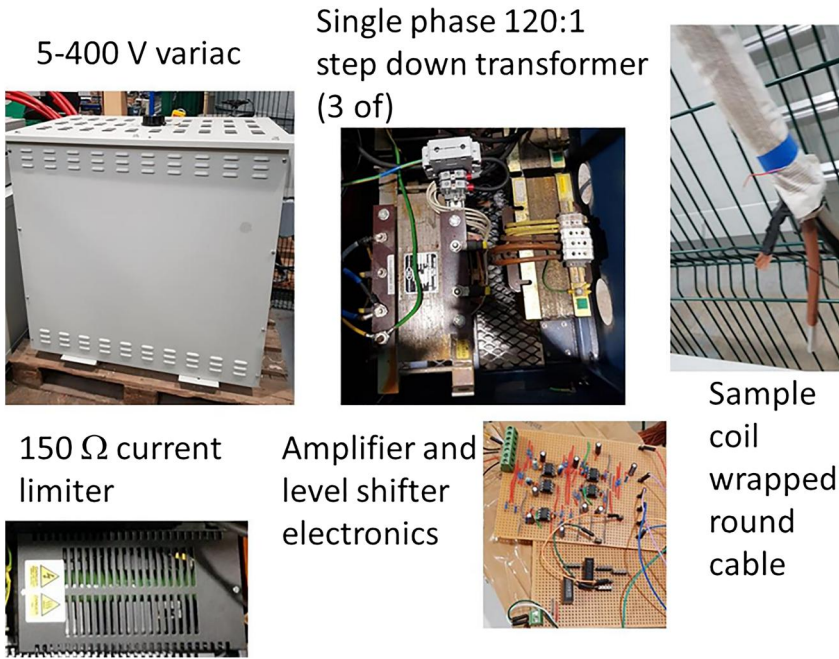


FIGURE 9 A photo collage of the test setup

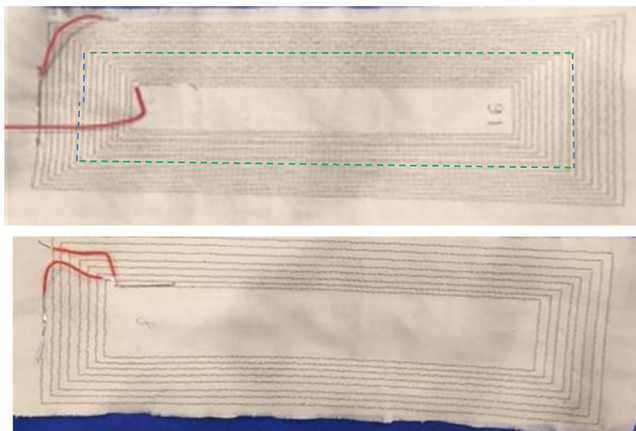


FIGURE 10 Photographs of the textile sensors coils with 16 turns and 8 turns. The dashed green lines indicate an 'averaged' coil

digital converter (MCP3008 chip) which uses a serial line to the Raspberry Pi (this does not have analogue inputs). Raspberry Pi removes the dc offset and post-processes the values and passes this to a central server via a GPRS dongle.

In this study, results only from the scope probes are analysed. The A2D converter will add additional uncertainty to the final product. The current probe and a voltage probe connected to the amplified and shifted emf were connected to a Teledyne Lecroy HDO6104 Oscilloscope to capture the measurements. The directly measured current was used to validate the indirect current measurement using the sensor.

The conductive thread (Madeira HC40 $<300 \Omega/\text{m}$ silver-plated polyamide) was sewn onto fabric (medium-weight calico in the prototyping stage) using an embroidery machine (Brother PR1050x 10-needle). Sample textile sensors with different numbers of turns of conductive thread were produced as shown in Figure 10. These were aligned with the longest edge

against a tape marker indicating the position of the red phase conductor. The dimensions of the textile coils were recorded and used in excel with Equations (6), (11) and (12) to calculate the mutual inductance, which was then used to estimate the load current in conjunction with the measured voltage. The load current was separately recorded on a single phase using a current probe connected to the scope for validation.

4 | RESULTS

The calculated mutual inductance between each conductor and coil as its position around the conductor changes for each of the samples is shown in Figures 11–13. The mutual inductance between each and the coil conductor (M_{RC} , M_{YC} and M_{BC}) varies as the coil rotates around the conductor.

The mutual inductance has rotational symmetry as expected. As the coil's position aligns with each conductor in turn, it reaches close to a peak and is higher as the number of turns increases.

The current varied for each sample and the measured current and voltage waveforms were captured. An example of the captured current and voltage for the 16 turns sample at 109 A rms are shown in Figure 14 and Figure 15. The measured rms current was plotted against the calculated rms current from (14) using the measured voltage in Figure 16 for each of the samples (8 turns, 12 turns and 16 turns).

An alternative to the Neumann method is to look at an 'average' coil. An 'average' coil refers to a coil of the same number of windings as the distributed coil all of which have an average length that is located in the average position with respect to the conductors as shown by the green lines in Figure 10. The calculations are then simplified, as it is assumed that each turn is located at the same location.

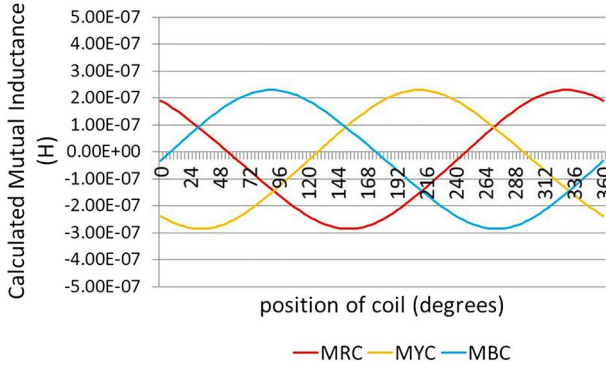


FIGURE 11 The calculated mutual inductance of the coil with each conductor with relation to the radial position of the coil with 8 turns

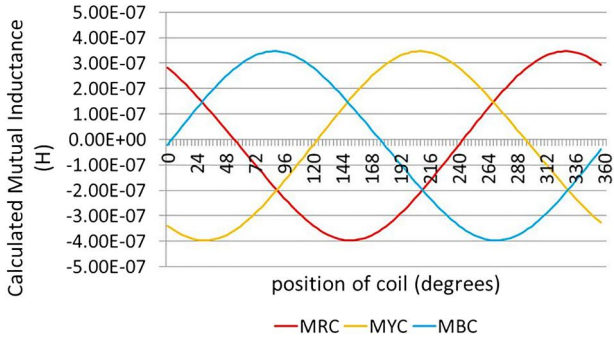


FIGURE 12 The calculated mutual inductance of the coil with each conductor with relation to the radial position of the coil with 12 turns

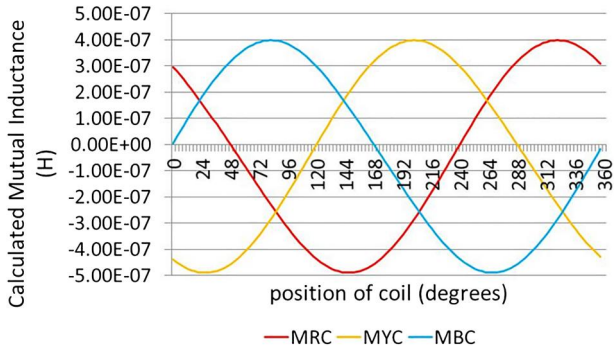


FIGURE 13 The calculated mutual inductance of the coil with each conductor with relation to the radial position of the coil with 16 turns

The graph of back calculated current against measured current for the averaged coil is shown in Figure 17

The offset error in the calculation in Figure 16 can be estimated using (15).

$$100 \times \frac{(\text{Measured rms current} - \text{Calculated rms current})}{\text{Measured rms current}} \quad (15)$$

This equates to around 14% between 10 and 110 A in Figure 16. The errors are made up of errors in the scope measurements and errors from the estimation of mutual

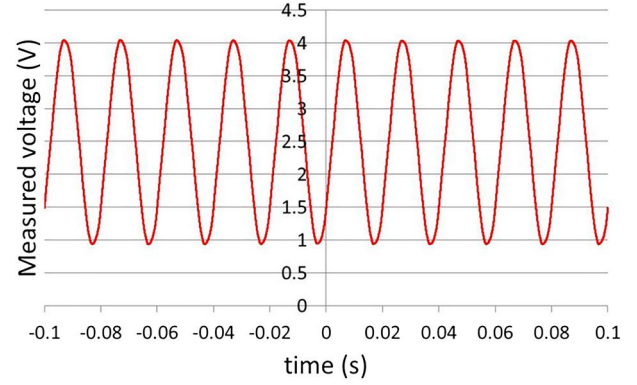


FIGURE 14 A plot of the amplified and level shifted coil voltage with time using the sensor with 16 turns with a current of 109 A rms captured on the scope

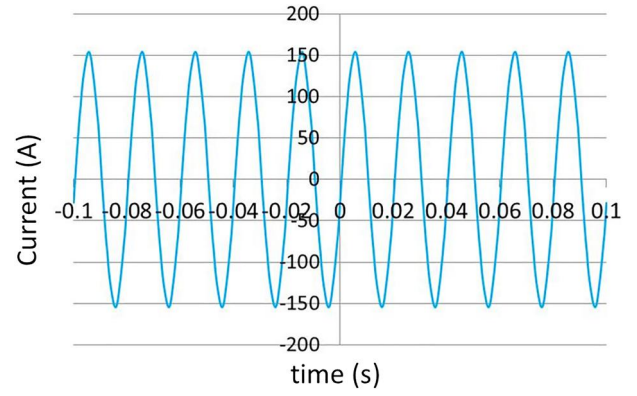


FIGURE 15 A plot of the current probe measured data with time with a current of 109 A rms, captured on the scope at the same time as the voltage in Figure 14

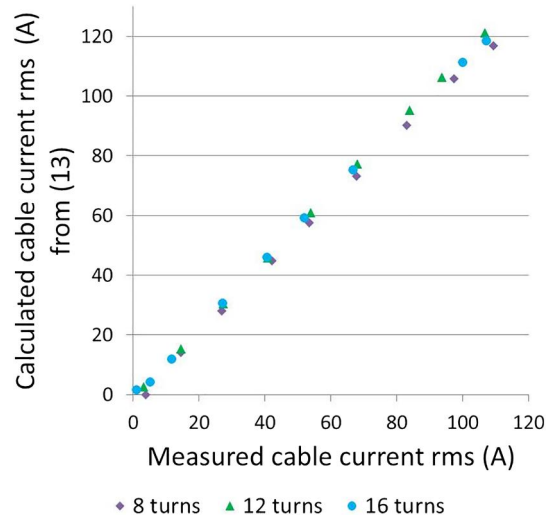


FIGURE 16 Graphs of measured cable current and calculated cable current from voltage measurements for different numbers of turns

inductance. The R^2 goodness of fit parameter is 0.9979 indicating that there is good linearity between the measured and calculated values.

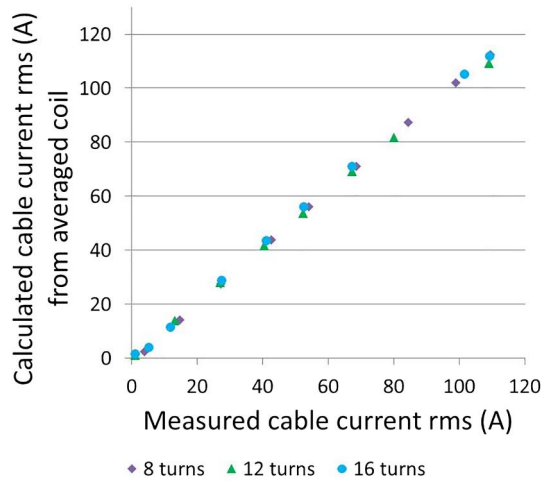


FIGURE 17 Graphs of measured cable current and averaged calculated cable current from voltage measurements for different numbers of turns

Both calculation methods yield close results. This is important for two reasons; it shows that the Neumann calculation can be used to back-calculate the current from the measured voltage from (13). It also shows that a complex turns arrangement can be represented by the number of turns of an average coil (average height and average arc around the conductor) to calculate current.

A comparison to current state-of-the-art sensors is shown in Table 2.

The laboratory equipment only goes as high as 120 A rms. The electronics have been designed to maximise the response to this range. However, as the system works like an air-cored transformer, there is no technical reason why the system should not work over the same range as the Siemens Rogowski coil. Minor amplifier adjustments would be required. There is no practical means of proving this at this time with the equipment available.

Further work is needed to identify sources of the offset. Also, caution is needed, as the results are dependent on the location of the coil with respect to the reference point. For example, Figure 18 shows the calculated emf induced in the coil (at 109 rms current) as a function of location with respect to the reference shown by the red line. This induced emf varies from just over 0.846–0.87 V depending on coil location. Any shift away from the reference line will result in an increase in emf for a given current.

One assumption within this research is that the current is balanced in the conductor. All results have been tested under balanced conditions only as there is no laboratory capability to test imbalance at this time. However, a theoretical current imbalance on one phase of the eight-turn coil at +10% leads an additional estimated uncertainty of up to +6%. Future work will look at using arrays of coils to allow imbalance to be calculated.

Additional assumptions include that the location of the coil in relation to the conductor is known, the op-amp circuitry is

TABLE 2 Comparison of textile coil to a Siemens Rogowski coil [34]

Performance criteria	Rogowski coil	Textile coil
Current range	5–4000 A	10–150 A (not tested above this range but expected to be 4000 A)
Voltage range of conductor	1000 V rms	3 V to 11 kV rms
Frequency	50/60 Hz	Only tested at 50 Hz
Accuracy	<0.6%	<14% with <6% with average coil method
Linearity	$\pm 0.2\%$	$\pm 0.3\%$
Temperature sensitivity	0.07% per °C	Not known
Phase error	<−0.5°	Not known
Ratio error	<0.6%	Not known
Location error	Up to 2% typical for Rogowski coils but not quoted in the data sheet	<4%
Cost for five-way substation	15 × 391 USD each = £5000 uninstalled cost	£150 installed

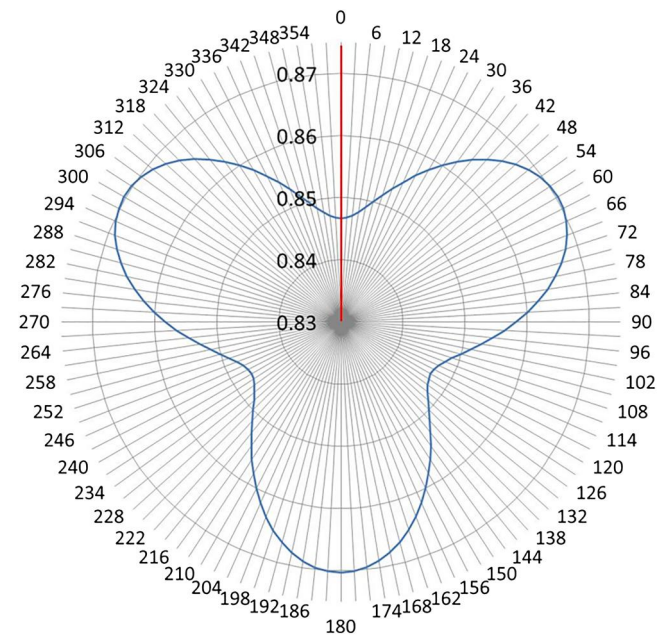


FIGURE 18 The calculated rms emf of a 12-turn conductor with radial coil location for a fixed current of 100 A rms

assumed to be ideal and there is no impact of noise, the frequency of the supply is fixed at 50 Hz. From Equation (14), the current is inversely proportional to frequency. The current will be lower if the frequency is increased. Therefore, using a fixed value of 50 Hz (as opposed to, e.g., a value of 50.05 Hz)

increases the estimate of load current by 0.1%. The textile coil has only been tested at a single frequency. A single different fundamental frequency could be dealt with under this setup by measuring this frequency and using this in the calculations giving similar levels of accuracy. The accuracy would be impacted with harmonics in the conductors, and an integrator in the electronics would be required along with better harmonic post processing to analyse this properly.

To improve accuracy, an integrator could be added to the electronics similar to that used in a Rogowski coil to include the frequency within the measurement. The impact of these assumptions will be to increase the measurement uncertainty.

It is difficult to undertake transient analysis with the current rig setup because the method of controlling current through the variac is a manual dial, which is slow to turn relative to the grid frequency. Figure 19 shows the measured voltage when the current is switched on to a pre-set 109 A rms using a circuit breaker. The initial current is dependent on the X/R ratio of the circuit and the point on the voltage wave where the waveform is switched.

As the rate of change of current is higher at switch on, this results in an overshoot of the voltage (in this instance of 22%). The voltage takes seven cycles (140 ms) to recover to the expected value. It is anticipated that the sensor will be reporting values between 10 s and 15 min in the field (to avoid excessive communication costs); the error produced by such an extreme event will not be significant over the course of the reporting period.

Future work is planned to use this technique to look at unbalanced systems using multiple textile coils. A more detailed look at the impact on uncertainty will be undertaken at this time.

The average costs for eMS and Gridkey LV monitoring as reported by SP energy networks [35] averaged over a 100 11-kV/400-V substation installations is £3k per substation of which £1175k is the monitoring equipment. The cost of an equivalent textile-based solution based on 2021 prices is shown in Table 3.

Installation requires positioning and cable tying the sensor to the cable (around 10 min) and plugging in the box with the electronics to a 240 V plug socket.

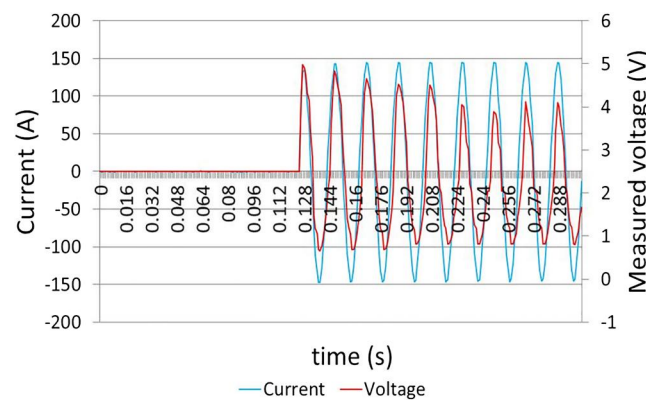


FIGURE 19 The transient response of the sensor to the current being switched to 109 A rms, using the 16-turn coil

TABLE 3 Costs of textile monitoring system

Component	Unit cost	No. units	Total cost
Conductive thread, e.g. Maderia HC40 conductive thread	£37.61/250 m	8 m	£1.20
Material base (any non-stretch fabric)	£3/m ²	20 × 30 cm	£0.20
Raspberry Pi 4	£33.90	1	£33.90
Bespoke PCB board	£4	1	£4
Portable dongle, e.g. Huawei E1750 3G	£15	1	£15
Enclosure for components, e.g. Farnell 2499448	£12.82	1	£12.82
Power supply TOOGOO AC 100 V~240 V to dc 5 V 3 A 15 W power	£5.69	1	£5.69
MCP3008 chip, e.g. RS 738-6651	£1.67	1	£1.67
Op Amp chips, TLC2272 and TLC 272	£1.57 & 0.84	1 each	£2.41
Resistors and capacitors (various)	Approx. £5/100		£5
Total			£81.89

5 | CONCLUSION

Large-scale roll out of low-voltage substation monitoring using Rogowski coil monitoring technology is not possible as it is too expensive. This study described a new method of using a low-cost textile-based coil to estimate the load current at a substation on a three-phase cable with an earthed shield.

The method relies on knowing the dimensions of the coil and calculating the mutual inductance between the coil and the conductors in the cable using Neumann's method to account for the complex geometry.

A simplification of the complex geometry using a multi-turn coil of average height and positioning also yields results which are suitable. Additional improvements could be realised by modelling the conductor as a group of filaments (known as the mesh-matrix method).

The experimental results from three different textile-based coils of different numbers of turns and dimensions were used to show a comparison between directly measured current and calculated current.

The disadvantage of this sensor is that there is 14% offset error in the result between 10 and 190 A, but the system shows good linearity of <0.3% error. Pre-calibration could be used to help with correcting the offset. The error from this new sensor is much higher than that with the current technology, but there is scope for improvement as this research is at an early stage. The advantage of this method is that its cost is much lower than that of commercially available products and could provide large-scale monitoring to a lower degree of accuracy to help show where low-voltage substations have time varying spare capacity. There is no perceivable difference caused by using different numbers of turns, so these can be adjusted to suit the application.

The techniques developed in this study lend themselves to the use of multi-coil sensors as a means of establishing unbalanced currents. Future work will focus on dealing with the imbalance and then applying other techniques in literature such as auto-calibration to develop a low-cost rugged sensor that can be easily wrapped around a sensor in tight places.

ACKNOWLEDGEMENTS

The authors would like to acknowledge the EPSRC grant EP/N032888/1 for helping to fund this study.

DATA AVAILABILITY STATEMENT

The data that support the findings of this study are available from the corresponding author upon reasonable request.

ORCID

Mina Abedi Varnosfaderani  <https://orcid.org/0000-0003-2890-3810>

REFERENCES

1. eMS: Low voltage. <http://www.emsni.com/market-sectors/low-voltage/#>. Accessed 27 May 2020
2. Gridkey: All products. <https://www.gridkey.co.uk/all-products/>. Accessed 27 May 2020
3. Nortech: LV substation monitoring. <https://nortechonline.co.uk/applications/lv-substation-monitoring/>. Accessed 27 May 2020
4. Xiang, Y., et al.: A novel contactless current sensor for HVDC overhead transmission lines. *Sensors J. IEEE*. 18(11), 4725–4732 (2018)
5. Sun, X., et al.: Noncontact operation-state monitoring technology based on magnetic-field sensing for overhead high-voltage transmission lines. *IEEE Trans. Power Del.* 28(4), 2145–2153 (2013)
6. Sun, X., et al.: Overhead high-voltage transmission-line current monitoring by magneto-resistive sensors and current source reconstruction at transmission tower. *IEEE Trans. Magn.* 50(1) (2014)
7. Khawaja, A.H., et al.: Estimation of current and sag in overhead power transmission lines with optimized magnetic field sensor array placement. *IEEE Trans. Magn.* 53(5), 6100210 (2017)
8. Bernieri, A., et al.: An AMR-based three-phase current sensor for smart grid applications. *IEEE Sensors Journal*. 17(23), 7704–7712 (2017)
9. Wu, J., et al.: A novel low-cost multicoil-based smart current sensor for three-phase currents sensing of overhead conductors. *IEEE Trans. Power Deliv.* 31(6), 2443–2452 (2016)
10. Moghe, R., Lambert, F., Divan, D.: A novel low-cost smart current sensor for utility conductors. *IEEE Trans. Smart Grid*. 3(2), 653–663 (2012)
11. D'Antona, G., et al.: Processing magnetic sensor array data for AC current measurement in multiconductor systems. *IEEE Trans. Instrum. Meas.* 50(5), pp. 1289–1295. (2001)
12. Chirtsov, A., Ripka, P., Grim, V.: Three-phase busbar current transducer. *Magn. Lett. IEEE*. 10, 1–5. 8110805 (2019)
13. Wang, P., et al.: Planar Rogowski coil current transducer used for three-phase plate-form busbars. In: *IEEE Instrumentation & Measurement Technology Conference IMTC*, Warsaw, pp. 1–4. (2007)
14. Wang, P., Zhang, G., Qian, Z.: A planar-coil-based current transducer used in distribution power system. *IEEE Trans. Instrum. Meas.* 59(11), 3028–3033 (2010)
15. Chen, K.L., Chen, N.M.: A new method for power current measurement using a coreless Hall effect current transformer. *IEEE Trans. Instrum. Meas.* 60(1), 158–169 (2011)
16. Geng, G., et al.: Noninvasive current sensor for multicore cables. *IEEE Trans. Power Deliv.* 33(5), 2335–2343 (2018)
17. Geng, G.C., et al.: Contactless current measurement for enclosed multiconductor systems based on sensor array. *IEEE Trans. Instrum. Meas.* 66(10), 2627–2637 (2017)
18. Itzke, A., et al.: The influence of interference sources on a magnetic field-based current sensor for multiconductor measurement. *IEEE Sensors J.* 18(16), 6782–6787 (2018)
19. Zhu, K., et al.: On-site non-invasive current monitoring of multi-core underground power cables with a magnetic-field sensing platform at a substation. *IEEE Sensors J.* 17, pp. 1837–1848. (2017)
20. Zhu, K., Liu, X., Pong, P.W.T.: On-site real-time current monitoring of three-phase three-core power distribution cables with magnetic sensing. *IEEE Sensors*. 1–4 (2018)
21. Zhu, K., Pong, P.W.T.: Curved trapezoidal magnetic flux concentrator design for current measurement of multi-core power cable with magnetic sensing. *IEEE Trans. Magn.* 55(4), 1–9 (2019)
22. Yamashita, T., et al.: Development of thin film based flexible current clamp sensor using screen-printed coil. *Microsyst. Technol. Micro. Nanosyst. Infor. Storage Process. Syst.* 22(3), 577–581 (2016)
23. Strickland, M., et al.: Low cost current measurement of three phase cables. In: *Universities Power Engineering Conference (UPEC)*, Glasgow, pp. 1–6. (2018)
24. Strickland, D., et al.: Low cost 11 kV network 3 phase cable current measurement using a novel coil device. In: *IEEE Power & Energy Society General Meeting (PESGM)*, Atlanta, pp. 1–5. (2019)
25. Yip, M.C., Niemeyer, G.: High-performance robotic muscles from conductive nylon sewing thread. In: *IEEE International Conference on Robotics and Automation*, Washington, pp. 2313–2318. (2015)
26. Paraskevopoulos, A., et al.: Higher-mode textile patch antenna with embroidered vias for on-body communication. *IET Microw. Antennas Propag.* 10(7), 802–807 (2016)

27. Chauraya, A., et al.: Addressing the challenges of fabricating microwave antennas using conductive threads. In: 6th European Conference on Antennas and Propagation, Prague, pp. 1365–1367. (2012)
28. Hughes-Riley, T., Dias, T., Cork, C.: A historical review of the development of electronic textiles. *Fibers*. 6, 34 (2018)
29. Mikkonen, J., Townsend, R.: Frequency-based design of smart textiles. In: Proceedings of the 2019 CHI Conference on Human Factors in Computing Systems, CHI'19, Paper 294, pp. 1–12. ACM, New York (2019)
30. Aigner, R., et al.: Embroidered resistive pressure sensors: A novel approach for textile interfaces. In: Proceedings of the 2020 CHI Conference on Human Factors in Computing Systems, CHI '20, Honolulu, HI, USA, pp. 1–13. (2020)
31. Williamson, S., Mueller, M.A.: Induction motor end winding leakage reactance calculation using the Biot-Savart method, taking rotor currents into account. In: Proceedings of ICEM'90, Boston, pp. 480–486. (1990)
32. Sonntag, C.L.W., Lomonova, E.A., Duarte, J.L.: Implementation of the Neumann formula for calculating the mutual inductance between planar PCB inductors. In: Proceedings of the 2008 Int. Conference on Electrical Machines, Vilamoura, pp. 1–6. (2008)
33. Liu, S., Su, J., Lai, J.: Accurate expressions of mutual inductance and their calculation of Archimedean spiral coils. *Energies*. 12 (2019)
34. Siemens: Technical Specification Sheet Document, No.149-405, Rogowski Coil Flexible Current Transformers. <https://www.downloads.siemens.com/download-center/Download.aspx?pos=download&fct=getasset&id1=A6V10398427>. Accessed 5 Jan 2021
35. SP Energy Networks: Flexible Networks for a Low Carbon Future. https://www.spenergynetworks.co.uk/userfiles/file/CostBenefitAnalysis_EnhancedNetworkMonitoring03.pdf. Accessed 27 May 2020

How to cite this article: Strickland, D., et al.: Textile-based sensors for electrical current measurement in three-phase cables. *IET Smart Grid*. 5(1), 1–11 (2022). <https://doi.org/10.1049/stg2.12047>